Resonance Raman Investigations of Cytochrome $P450_{CAM}$ from *Pseudomonas putida*

P. M. Champion,*[1a] I. C. Gunsalus,[1b] and G. C. Wagner[1b]

Contribution from the Chemistry Department, Baker Laboratory, Cornell University, Ithaca, New York 14853, and the Biochemistry Department, Roger Adams Laboratory, University of Illinois, Urbana, Illinois 61801. *Received September 2, 1977*

Abstract: Resonance Raman spectra of the hemeprotein cytochrome $P450_{CAM}$ in several stable reaction states are obtained with laser excitations in the Soret region (350–450 nm). Resonance in the Soret region yields vibrational modes of greatly enhanced intensity resulting from the large transition moments associated with the absorption band. The oxidized cytochrome, in the substrate-free ferric form, displays a selective enhancement of vibrations at 676 and 1372 cm^{-1} assignable to normal coordinates of expansion for the porphyrin in the excited state. The substrate bound cytochrome in both the oxidized and reduced states displays unusual peak positions indicative of a weakening in porphyrin ring bond strengths. This effect is interpreted as an increase in the population of the π^* antibonding orbitals of the porphyrin ring resulting from the interaction of a strongly electron-donating axial ligand (such as the mercaptide sulfur of cysteine). The Raman spectra, which are also found to be sensitive to spin-state equilibria, show predominantly low-spin ferric heme in the substrate-free cytochrome and a mixture of high- and low-spin ferric heme in the substrate complex. Addition of the effector protein putidaredoxin to the camphor complexed cytochrome shifts the spin-state equilibrium toward a low-spin form. The Raman spectral properties of native $P450_{CAM}$ are further elucidated by comparison to the spectra of a native ^{34}S-labeled sample and to the acetone inactivated "P420" state. Raman spectra of hemeproteins in vivo are demonstrated with resonance excitation in the Soret region of intact *P. putida* cells. The Soret excited Raman spectra of cytochrome $P450_{CAM}$ and chloroperoxidase are remarkably similar and differ from those of horseradish peroxidase.

Cytochromes P450, a term first assigned to protein with an intense absorption band near 450 nm in dithionite reduced, CO-complexed liver microsomes,[2,3] were subsequently associated with a new class of hemeproteins containing the dissociable prosthetic group iron protoporphyrin IX. These b-type P450 hemeproteins catalyze the monoxygenase or "mixed-function" oxidase reactions utilizing a two-electron reduction of dioxygen coupled with hydrocarbon oxygenation. In the last 20 years, cytochrome P450 monoxygenases have been found to comprise an ubiquitous class of hydroxylase systems, multiple in number and diverse in substrate selectivity, that are associated with a broad spectrum of biological functions. Included in this class are the membrane bound mammalian systems mediating synthetic steroid hydroxylations for hormonal activation within the adrenal cortex mitochrondria[4] and the degradative or assimilatory hydroxylations of toxic, carcinogenic, and drug-related compounds within the liver microsomes.[5-8] A soluble three-component P450 monoxygenase system, the camphor 5-monoxygenase [EC. 1.14.15.1], has been identified and purified from *Pseudomonas putida* by Gunsalus and co-workers.[9-11] Of all P450 cytochromes the bacterial $P450_{CAM}$, or cytochrome *m*,[12] has been the most extensively characterized, including energetics and reaction dynamics in the monoxygenase cycle[13] and the physical and resonance properties of the heme active site.[14] This system catalyzes the hydroxylation of the bicyclic monoterpene camphor (2-bornanone) to the 5-exo alcohol as shown by the reaction cycle in Figure 1. The three purified components, an FAD flavoprotein, putidaredoxin reductase (fp), an iron–sulfur protein of the $Fe_2S_2^*Cys_4$ class, putidaredoxin (Pd), and a b-type hemeprotein, cytochrome *m* (*m*), can be combined to achieve a fully active enzyme system. Cytochrome *m* binds the substrate D(+)-camphor and, after a one-electron reduction, molecular dioxygen O_2; cytochrome *m* and putidaredoxin participate in the product formation step coupled to a second one-electron reduction. The profound similarity in terms of structure, function, and catalytic cycle of cytochromes P450 has rendered the abundant and easily purified bacterial monoxygenase an effective analogue or biological model for molecular characterizations of a mixed-function oxidase.

Although a wide variety of physical techniques have been applied to cytochrome *m* of the camphor 5-monoxygenase system,[14] specific structural properties of the hemeprotein active site remain uncertain. In particular, the axial ligand that binds to the central iron atom has not been positively identified, although a mercaptide sulfur of cysteine has been suggested.[17-21] Furthermore, many physical techniques, e.g., Mössbauer spectroscopy,[22,23] magnetic susceptibility,[24] and electron paramagnetic resonance,[25] require experimental observation at cryogenic temperatures and millimolar concentrations, and thus the results require extrapolation into the physiological conditions. Optical absorption spectroscopy has thus remained a main tool for classification and characterization of cytochrome *m* and most other hemeproteins. However, resonance Raman spectroscopy is now rapidly developing into an important alternate probe of hemeproteins at ambient temperature.[26]

Resonance Raman spectroscopy utilizes an inelastic photon scattering process as a selective probe of molecular vibrations. This process differs from the normal Raman effect by the intensity enhancement of the scattered radiation as the excitation frequency approaches the energy of an electronic transition. Thus, excitation frequencies close to the visible (α, β) or ultraviolet (γ or Soret) absorption bands of a hemeprotein detect selectively certain vibrational modes of the heme group. In resonance, large enhancements of the Raman vibrational modes are achieved and the intensity, energy, and polarization of the scattered radiation contain information about the structure and symmetry of the heme group and the composition of the resonant absorption bands.[27,28]

The Soret and α bands arise from allowed π–π^* transitions of the porphyrin aromatic system. Configuration interaction mixes these states, however, to give the Soret band almost an order of magnitude more intensity than the α band.[29] Further mixing through vibronic coupling generates the β band which has been shown to contain individual vibronic components of the excited state (Q_{0-1} transitions) that correspond to observed (ground state) Raman modes.[27,30]

Resonance excitation in the absorption bands of hemeproteins generates two basic types of Raman scattering that can be classified as A-term and B-term activity.[31] The activity associated with an A term involves resonance with only a single electronic state and derives intensity from mixed Franck–Condon overlaps arising from shifts in the excited state equi-

0002-7863/78/1500-3743$01.00/0

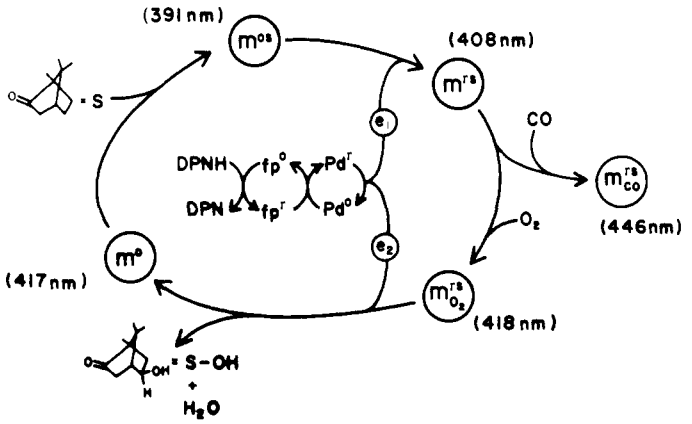

Figure 1. Cytochrome $P450_{CAM}$ reaction cycle. Cytochrome P450 is abbreviated *m* for monoxygenase in order to simplify labeling of ligand and redox states; m^{o}, ferric cytochrome; m^{os}, ferric $P450_{CAM}$-substrate complex; m^{rs}, ferrous $P450_{CAM}$-substrate complex; $m^{rs}_{O_2}$, oxygenated ferrous $P450_{CAM}$-substrate complex; m^{rs}_{CO}, carbon monoxide ferrous $P450_{CAM}$-substrate complex; DPNH, pyridine nucleotide; fp, flavoprotein putidaredoxin reductase; Pd, putidaredoxin. The reaction states are also labeled by the wavelength of their Soret maxima.

librium position and/or changes in the shape of the excited state potential energy well.[31] Raman activity associated with modes involved in vibronic mixing of two electronic states, as in the β band, are classified as B-term active.[31] The intensity of the B-term modes depends upon the product of the transition dipole moments of the electronic states being mixed, while intensity of the A-term modes depends upon the square of the transition moment of the single electronic state in resonance. Thus, resonance with the visible bands of hemeproteins usually yields predominantly B-term Raman modes (the A-term scattering is reduced owing to the relative weakness of the α transition); on the other hand, resonance with the Soret transition will bring out strong A-term scattering.

Until recently, most Raman experiments on hemeproteins utilized the readily available visible laser radiation, with resonance excitation within the α and β bands. In this study we demonstrate the first use of deep blue and near ultraviolet excitation wavelengths to achieve *direct* resonance with the Soret band of a hemeprotein. Soret excitation serves the dual purpose of moving the Raman spectrum to the blue of the broad visible fluorescence band ($\lambda_{max} \sim 540$ nm) associated with P450 samples and of increasing the intensity of the Raman scattering via the large resonance transition moments present in the Soret band. We have recently reported preliminary resonance Raman spectra of cytochrome $P450_{CAM}$[32] which demonstrate that high-quality Raman spectra can be obtained by using a laser excitation wavelength (363.8 nm) near resonance with the Soret absorption band of m^{os}. The present work extends these efforts to include other reaction states and chemical complexes pertinent to the camphor-5-monoxygenase reaction cycle. In addition, we introduce a variety of laser excitation wavelengths in the Soret region as a means of achieving a better understanding of the subtle and complex Raman spectra. Figure 2 illustrates the electronic absorption spectra in the Soret region for various oxidation and ligand states of cytochrome *m*, along with the respective laser excitation wavelengths utilized in this study.

Experimental Section

Materials. Cytochrome *m* and putidaredoxin are isolated in pure form from the freeze-thaw autolytic mutant of *Pseudomonas putida*, strain PpG 786 (ATCC 29607), as previously described.[33] The nonautolytic parent, strain PpG 1 (ATCC 17453), is examined for studies on intact cells. The proteins isolated from the two strains, grown on D(+)-camphor, are equivalent by physical-chemical criteria.[11] Camphor free cytochrome *m* (m^{o}) is prepared from the m^{os} form by Sephadex G-15 chromatography as described elsewhere.[33] Reduction of m^{os} is accomplished with a slight excess of sodium dithionite (Hordman and Holdman, Manchester, England). A catalytically inactive form of cytochrome *m*, referred to as P420, is prepared by treating an aliquot with acetone (30% v/v) for 1 h at room temperature.[34] Horseradish peroxidase and chloroperoxidase prepared by previously described procedures[35] are generously provided by Dr. L. P. Hager.

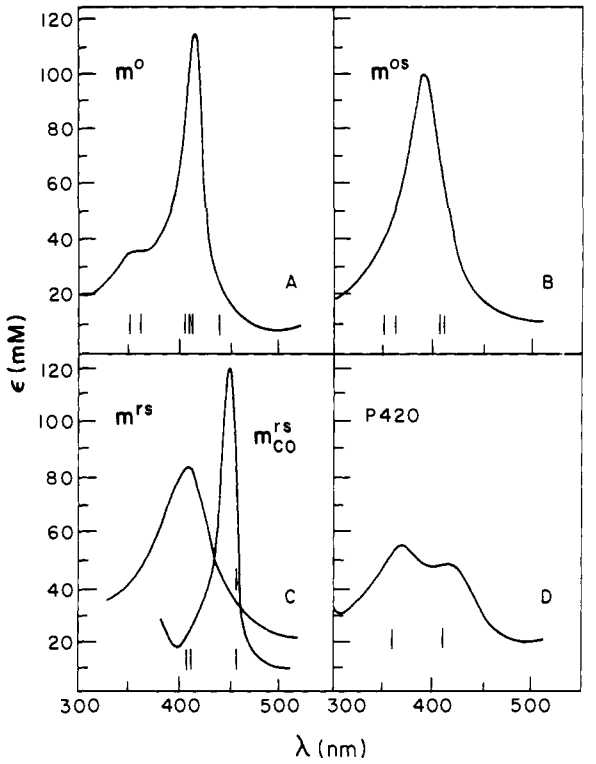

Figure 2. The absorption spectra in the Soret region of some of the complexes under study in this investigation. The short vertical lines represent the laser excitation wavelengths used to obtain Raman spectra. A, m^{o}; B, m^{os}; C, m^{rs} and m^{rs}_{CO}; D, P420 (oxidized).

Methods. The Raman samples of cytochrome *m* are prepared in 0.1 M potassium phosphate pH 7.0; substrate, when present, is 250 μM D(+)-camphor. The putidaredoxin samples are in 25 mM Tris·Cl pH 7.4, containing 5 mM 2-mercaptoethanol; the Pd^{o}·m^{os} complex contains 1.25 mM D(+)-camphor and 0.25 M KCl. Final protein concentrations are adjusted to give an absorbance of unity near the Soret maximum in a 2-mm path length Raman sample cuvette; typical concentrations are 50–100 μM for cytochrome *m* and 500 μM for putidaredoxin. The optical absorption of each sample is routinely checked with a Cary 14 spectrophotometer before and after each Raman experiment to confirm that sample deterioration has not occurred. The Raman measurements are taken on samples maintained at approximately 4 °C by means of a thermoelectric cooling unit.

Two different lasers are employed: a Coherent Radiation Model CR 12 argon ion laser supplies the ultraviolet (351.1, 363.8 nm) radiation and a Spectra Physics Model 171 krypton laser provides excellent single line stability and power in the deep blue (406.7, 413.1, 415.4 nm). The laser light is filtered, when necessary, and focused onto the aqueous samples in a right angle scattering geometry. For the highly scattering bacterial cell paste an acute angle geometry is employed. Laser power measured at the sample is maintained near 20 mW. The polarization of the Raman scattered light is determined with a Polaroid filter, and a polarization scrambler ensures equal response of the monochromator to both polarizations. The Raman data are collected by means of a Spex 1401 double monochromator equipped for photon counting and digital storage capacity. This monochromator is calibrated before each run using the known wavelengths of an argon or krypton laser; care is taken to allow the monochromator lead screw to come to working temperature before making any measurements. The Raman spectra are averaged to reduce statistical fluctuations and plotted using a small computer.

Table I. Resonance Raman Peak Positions of P450 Complexes

m^{os} $\Delta\nu$(I, pol)[a]	m^{o} $\Delta\nu$(I, pol)	m^{rs} $\Delta\nu$(I, pol)	P420 $\Delta\nu$(I, pol)	m^{os} $\Delta\nu$(I, pol)	m^{o} $\Delta\nu$(I, pol)	m^{rs} $\Delta\nu$(I, pol)	P420 $\Delta\nu$(I, pol)
311 (w,u)				1342 (w,u)	1343 (w,u)		
318 (w,u)				1368 (s,p)		1344 (s,p)	
		332 (w,p)		1372 (s,p)[b]	1372 (s,p)	1361 (v,p)	1372 (s,p)
342 (m,p)	345 (m,p)		345 (m,u)	1380 (sh,u)			1382 (sh,u)
351 (m,p)				1396 (sh,dp)	1395 (w,dp)	1391 (s,dp)	1400 (w,u)
		362 (w,p)		1422 (sh,u)			
377 (m,p)	378 (m,p)	375 (w,p)		1429 (m,u)	1432 (w,u)	1425 (s, dp)	1430 (m,u)
		403 (w,p)			1464 (w,u)	1445 (sh,u)	1468 (w,u)
421 (w,p)	425 (w,p)	416 (w,p)		1488 (m,p)		1466 (s,p)	1490 (m,u)
675 (m,p)	676 (s,p)	673 (m,p)	676 (s,p)	1502 (sh,p)	1502 (m,p)		1502 (w,u)
691 (w,u)		692 (sh,u)		1526 (w,p)			1525 (m,u)
716 (w,u)		713 (w,dp)	715 (w,u)			1534 (s,dp)	
721 (w,u)			736 (w,u)	1550 (m,u)	1550 (sh,u)		1548 (sh,u)
754 (m,dp)	751 (m,dp)	745 (m,dp)	752 (w,dp)	1570 (s,p)	1560 (m,u)	1563 (s,p)	1570 (s,u)
784 (w,u)		783 (w,dp)		1581 (sh,p)	1581 (m,u)	1584 (s,p)	1585 (m,u)
796 (w,u)	797 (w,u)				1601 (m,p)		
821 (w,u)		815 (w,p)			1619 (m,p)		
	930 (w,p)	925 (w,u)		1623 (s,dp)	1635 (s,dp)	1601 (s,dp)	1627 (s,dp)
970 (sh,u)						1612 (sh,u)	
984 (w,u)	987 (w,u)	974 (m,u)			2049 (w,u)		
1004 (w,p)	1006 (w,u)	1000 (m,p)					
1086 (w,u)	1087 (w,u)	1080 (w,p)	1070 (w,u)				
		1115 (w,p)					
1125 (m,u)	1128 (m,p)	1125 (sh,p)	1125 (m,u)				
		1140 (w,u)					
1170 (m,u)	1170 (m,u)	1176 (m,dp)	1170 (w,u)				
1214 (sh,u)							
1225 (m,dp)	1223 (w,u)	1213 (m,dp)	1220 (sh,u)				
1232 (sh,u)	1245 (w,u)	1235 (sh,u)	1238 (w,u)				

[a] $\Delta\nu$ is Stokes shift in cm^{-1} (±2 cm^{-1}) relative to the excitation wavelength. I corresponds to relative intensity of peaks in the spectrum where they appear the strongest: s = strong, sh = shoulder, m = medium, w = weak, v = variable, pol refers to the polarization of peaks: p = polarized ($I_{\parallel}/I_{\perp} \lesssim 1/8$), dp = depolarized ($I_{\parallel}/I_{\perp} \sim 3/4$), u = undetermined. [b] Possibly due to a strongly enhanced low-spin fraction.

Results

Oxidized Camphor Complex, m^{os}. Representative Raman spectra of the substrate bound ferric heme enzyme, m^{os}, are shown in Figure 3. Marked differences in the spectra occur, particularly in the region below 500 cm^{-1}, as the laser excitation is applied to the blue (351.1 and 363.8 nm) and to the red (406.7 and 413.1 nm) sides of the Soret maximum (λ_{max} 391 nm). The 351-cm^{-1} mode, most prominent on 363.8-nm excitation, disappears completely at 413.1-nm excitation and is replaced by low-frequency modes at 342, 377, and 421 cm^{-1}. The modes above 500 cm^{-1} also exhibit substantial variation in relative intensities as the laser excitation frequency is moved across the Soret region. Excitation at the lower energy side of the Soret absorption results in an increase in relative intensities of the 675-, 1368–1372-, and 1488-cm^{-1} modes with an accompanying decrease in the 1623-cm^{-1} mode. The main porphyrin ring modes expected above 1300 cm^{-1} are predicted to be sensitive to the spin and oxidation state of the heme iron.[26] As we reported previously,[32] the positions of the three marker bands[26,36] (I at 1368 cm^{-1}, II at 1488 cm^{-1}, and V at 1623 cm^{-1}) are rather atypical. Particularly interesting in the present study is the apparent shift of band I from 1368 to 1372 cm^{-1} as the laser excitation is moved to the low-energy side of the Soret band. We believe that this phenomenon arises from a low-spin species with an unusually intense 1372-cm^{-1} mode when excited at 413.1 nm (e.g., see the spectra of m^{o}, Figure 5). The peak positions and intensities of the spectra in Figure 3 are summarized in Table I.

Preliminary results of Raman experiments on ^{34}S-labeled cytochrome m^{os} are focused on the spectral region between 665 and 700 cm^{-1}, since the 691-cm^{-1} mode has been implicated as a potential C–S stretching vibration of cysteine.[32] A larger than usual fluorescence background in this ^{34}S-labeled sample required the accumulation of multiple spectra to enhance the signal-to-noise ratio. Direct comparison of spectra from ^{34}S-labeled (enrichment >90%) m^{os} and ^{32}S-labeled (natural abundance) m^{os} does not confirm the assignment of the 691-cm^{-1} peak suggested earlier; the expected shift of 5 cm^{-1} to lower energy is not observed in the ^{34}S-labeled sample.

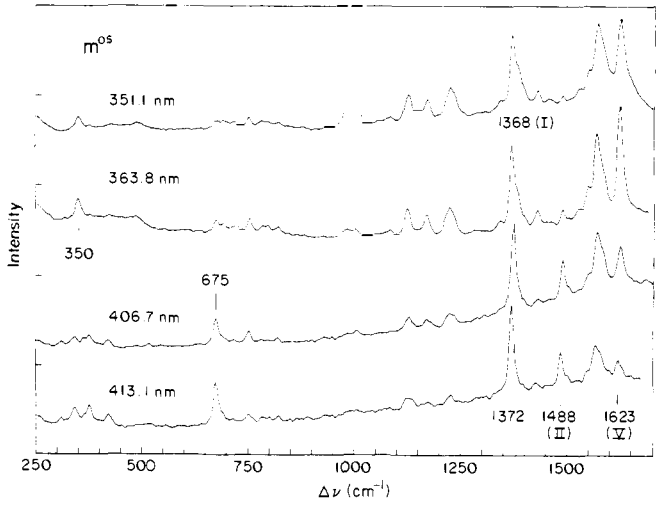

Figure 3. Resonance Raman spectra of the m^{os} complex. Slit widths are 5 cm^{-1} and counting time is 10 s/channel, 2 cm^{-1} step size. Excitation at 351.1 nm, 0–11K counts, unpolarized; 363.8 nm, 0–5K counts, unpolarized; 406.7 nm, 0–4K counts, unpolarized; 413.1 nm, 0–2.5K counts, parallel polarized. The truncated peak at 990 cm^{-1} is due to leakage of the 363.8-nm laser line through the optical filter. Each spectrum has its respective count range extended to the same height; origins are displaced for convenience.

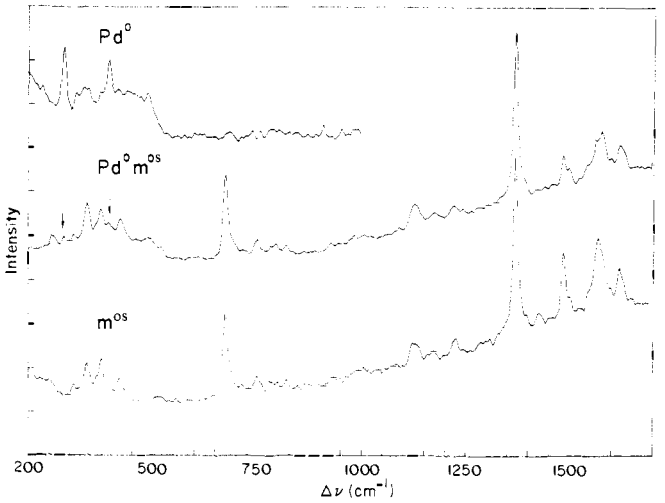

Figure 4. Resonance Raman spectra of cytochrome m^{os}, putidaredoxin Pd°, and a Pd°m^{os} complex. Same experimental conditions as those used in Figure 3. Pd°, 413.1-nm excitation, 0-2.2K counts, parallel polarized scattering; Pd°m^{os} complex, 413.1-nm excitation, 0-7K counts, parallel polarized scattering; m^{os}, 413.1-nm excitation, 0-2.5K counts, parallel polarized scattering. The arrows in Pd°m^{os} spectrum locate the strongest low-frequency putidaredoxin peaks. The count ranges are again equally expanded and displaced.

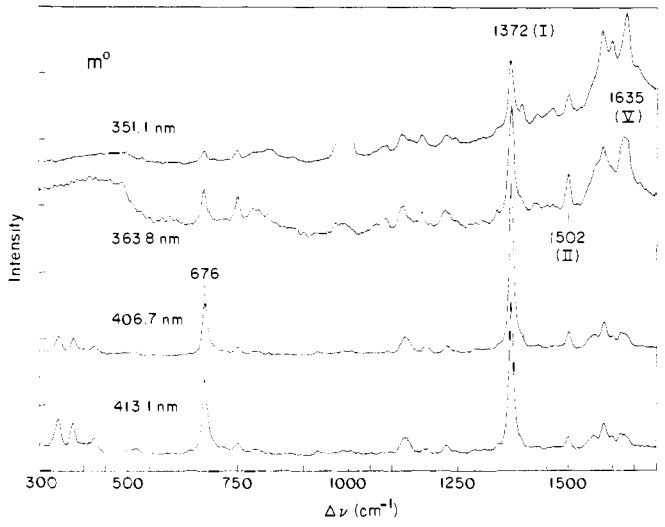

Figure 5. Resonance Raman spectra of the m^{o} complex. Experimental conditions as in Figure 3. Excitation at 351.1 nm, 0-12K counts, unpolarized; 363.8 nm, 0-2.5K counts, unpolarized; 406.7 nm, 0-18K counts, parallel polarization; 413.1 nm, 0-7K counts, parallel polarization. The count ranges are equally extended and the origins are displaced as in Figure 3. The truncated peak at 990 cm^{-1} is due to 363.8-nm laser radiation.

Previous equilibrium and dynamic studies[13] have demonstrated the formation of a stable putidaredoxin-cytochrome m^{os} dienzyme complex ($K_D \sim 2\ \mu M$) that functions in the camphor 5-monoxygenase reaction cycle. Figure 4 shows preliminary Raman measurements of a Pd°·m^{os} complex in addition to the individual components using 413.1-nm excitation. Raman spectra of ferric putidaredoxin, Pd°, in the low-frequency region display vibrational modes associated with the $Fe_2S_2^*Cys_4$ active center. The strongest vibrations are at 287 and 394 cm^{-1} and weaker modes appear between 300 and 350 cm^{-1}. The spectra of the Pd°·m^{os} complex (7:1) resolve the strong low-frequency iron-sulfur vibrations (arrows) of Pd° and the four low-frequency vibrations of m^{os}. An additional low-frequency mode is observed at 260 cm^{-1}. Above 500 cm^{-1} new peaks do not appear, although significant changes in relative intensities occur, particularly at 1490 cm^{-1} and in the 1550-1600-cm^{-1} region.

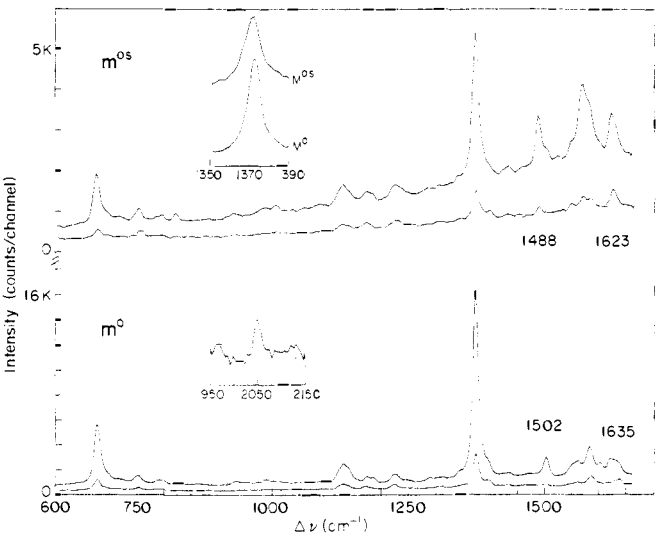

Figure 6. A comparison of the m^{os} and m^{o} Raman spectra. Slit widths, step size, and counting time as in Figure 3. m^{os}, 406.7-nm excitation, 0-5.5K counts, parallel (upper) and perpendicular (lower) polarized scattering; m^{o}, 406.7-nm excitation, 0-16K counts, parallel (upper) and perpendicular (lower) polarized scattering. The lower insert reveals the presence of a combination peak at ~2049 cm^{-1} while the upper insert compares the line shapes of the 1372-cm^{-1} peak of the two compounds.

Table II. Relative Intensity Variation of Raman Modes of m^{o}

	Excitation wavelength, nm				
	363.8	406.7	413.1	415.4	441.6
676-cm^{-1} mode	0.03[a]	1.2	1.3	1.4	0.04
1372-cm^{-1} mode	0.2	3.4	3.1	3.1	0.3

[a] Numerical values are a normalized measure of Raman intensity as explained in the text. Typical errors are ±15%.

Oxidized, Substrate-Free Cytochrome, *m*°. Figure 5 presents the Raman spectra of the substrate-free ferric heme cytochrome, m^{o}, measured with the same laser excitation wavelengths used with the m^{os} complex, Figure 3. The selective intensity enhancements observed earlier as the excitation wavelength is moved through the Soret region reappear. With excitation near the Soret maximum (λ_{max} 417 nm) enormous relative enhancement is seen in the 676- and 1372-cm^{-1} modes; the moderately intense low-frequency modes appearing at 345, 378, and 425 cm^{-1} with 413.1-nm excitation may also be quite significant. Marker band II located at 1502 cm^{-1} has a normal position for a low-spin ferric heme complex and with excitation at 351.1 nm the low-spin marker band V at 1635 cm^{-1} is clearly visible, though it is somewhat obscured by a 1619-cm^{-1} mode as the excitation approaches the Soret maximum. The peak positions and intensities displayed in Figure 5 are summarized in Table I.

A more quantitative exploration of the intensity variation of the 676- and 1372-cm^{-1} modes of m^{o} is shown in Table II. In these experiments the buffer solution contains 0.8 M SO_4^{2-}, a Raman intensity standard having a nonresonant vibrational mode at 980 cm^{-1}. The total area (parallel plus perpendicular polarization) of the 676- and 1372-cm^{-1} peaks determined at the various laser excitation frequencies is divided by the area of the corresponding 980-cm^{-1} peak and the ratios are displayed in Table II. The 676- and 1372-cm^{-1} modes undergo an order of magnitude increase in intensity as the excitation wavelength moves into the region of the Soret maximum. Since not all of the Raman modes are enhanced to this degree, as shown in Figure 5, the 676- and 1372-cm^{-1} modes appear to be rather unique in this respect.

Comparison of *m*^{os} and *m*°. Figure 6 allows a direct com-

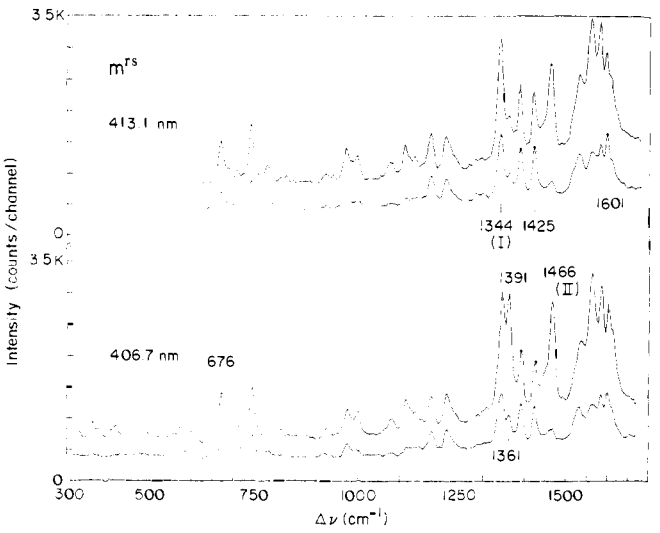

Figure 7. Resonance Raman spectra of the m^{rs} complex. Experimental conditions as in Figure 3. Excitation at 413.1 nm, 0–3.5K counts, parallel (upper) and perpendicular (lower) polarized scattering; 406.7 nm, 0–3.5K counts, parallel (upper) and perpendicular (lower) polarized scattering. The broad peaks at 470 and 580 cm^{-1} are due to scattering from the sodium dithionite used for reduction. The peak showing different intensities at 1361 cm^{-1} presumably is due to reduced P420.

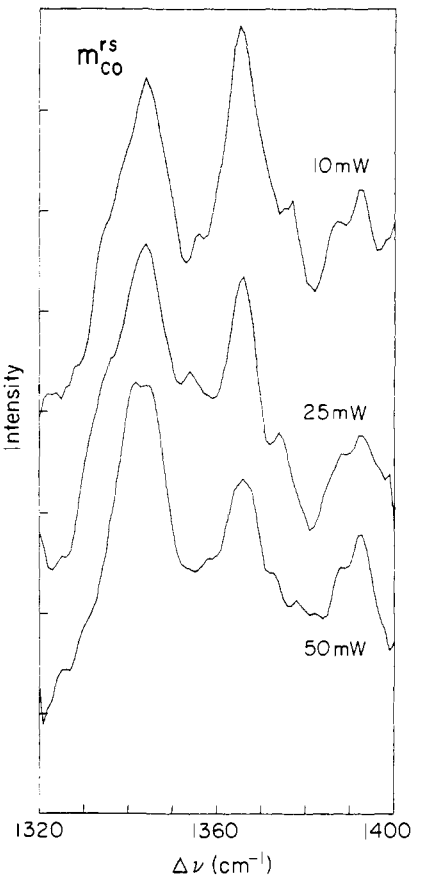

Figure 8. Resonance Raman spectra of the m^{rs}_{CO} complex taken with varying laser excitation powers. Excitation at 457.9 nm, unpolarized, with 10-, 25-, and 50-mW laser power. The peak at 1344 cm^{-1} is due to the m^{rs} complex, generated when the CO is photodissociated.

parison between the Raman spectra of m^{o} and m^{os}. The differences in absorption spectra of these two forms, as noted in Figure 2, should be considered when evaluating the strong relative intensities of the 676- and 1372-cm^{-1} modes in the Raman spectra of m^{o}, as well as the combination mode of these two intense vibrations at 2049 cm^{-1} shown in the lower insert. In the upper insert high-resolution spectra of the 1372-cm^{-1} peaks of both compounds are displayed. The peak shapes are definitely different and a shoulder or asymmetry is discernible around 1368 cm^{-1} in the m^{os} complex. Frequency shifts are also evident in the $m^{os} \rightarrow m^{o}$ conversion: band II moves from 1488 cm^{-1} in m^{os} to 1502 cm^{-1} in m^{o}, and band V from 1623 to 1635 cm^{-1}. In m^{os} the shift of band I to 1372 cm^{-1} and the shoulder of band II at 1502 cm^{-1} reveal a low-spin minority species in the sample.

Reduced, Camphor Complex, m^{rs}. Figure 7 shows polarized Raman spectra of the ferrous heme, camphor bound cytochrome, m^{rs}, with laser excitation near the Soret maximum (λ_{max} 408 nm). The polarization properties and intensity patterns of these spectra are unusual for a hemeprotein. The active vibrations of the heme chromophore in D_{4h} symmetry are A_{1g}, B_{1g}, B_{2g}, and A_{2g}. Typical values for the depolarization ratio,[37] ρ_l, for polarized (A_{1g}) $\rho_l \simeq 1/8$, depolarized (B_{1g}, B_{2g}) $\rho_l \simeq 3/4$, and anomalously polarized (A_{2g}) $\rho_l \gg 1$ modes have been observed for various hemeproteins[38a] with excitation in the visible region. Some polarized and depolarized peaks shown in Figure 7 for m^{rs}, however, have values of ρ_l slightly larger than expected. Most notable is marker band I at 1344 cm^{-1} (p) with $\rho_l \simeq 0.5$; the determination of $\rho_l \simeq 1/8$ for the polarized band II at 1466 cm^{-1} demonstrates the reliability of our experimental measurement of the depolarization ratio.

The m^{rs} marker bands also occur at anomalously low energies for a high-spin ferrous hemeprotein. The marker band I at 1344 cm^{-1} (p) is shifted 10–15 cm^{-1} to lower energy, and bands II at 1466 cm^{-1} (p) and V at 1601 cm^{-1} (dp) are each shifted approximately 5 cm^{-1} to lower energy.[39] The peak positions, polarizations, and intensities of the spectra in Figure 7 are summarized in Table I.

The 1361-cm^{-1} peak in Figure 7 is assigned to a heme impurity species, primarily in view of the variable intensity from one experiment to the next. A concomitant intensity variation of other peaks in the spectra is not observed (with the possible exception of the 676-cm^{-1} peak), implying that the remaining bands describe the native m^{rs} species. A prime suspect for the impurity species is a reduced P420 state of the cytochrome. The spectrum of an acetone inactivated P420 complex, in Figure 9 with 413.1-nm excitation, displays a strongly enhanced peak at 1360 cm^{-1} that could account for the impurity peak in Figure 7; the 675-cm^{-1} peak in the reduced P420 spectrum is quite likely masked underneath the 676-cm^{-1} peak of m^{rs}.

Reduced, Camphor Complex, CO Adduct, m^{rs}_{CO}. The CO adducts of ferrous P450, like those of hemoglobin and myoglobin, are photolabile. Thus, the accumulation of laser excited Raman spectra, especially with near-ultraviolet excitation wavelengths, is quite difficult. The problem has been partially overcome by monitoring the intensities of various Raman peaks as a function of laser power.[38] As more CO is photodissociated with increased laser power, the intensity of the m^{rs} spectrum is expected to increase and the intensity of the m^{rs}_{CO} spectrum to decrease. The results of such an experiment are displayed in Figure 8. Laser excitation at 457.9 nm employs relatively low energy photons yet maintains the fluorescence background within tolerable limits. Excitation with 10-mW laser power shows the largest contribution from the 1368-cm^{-1} mode which appears to be the m^{rs}_{CO} oxidation state marker band I. Excitation with 50-mW laser power reveals the presence of a relatively larger fraction of the m^{rs} species, with an oxidation state marker band I at 1344 cm^{-1}; excitation with 25-mW laser power displays relative intensities intermediate between those obtained with 10- and 50-mW power.

Acetone Inactivated m, "P420". Raman spectra of the oxidized and reduced states of an enzymatically inactive P420 species are given in Figure 9. The reduced state has been

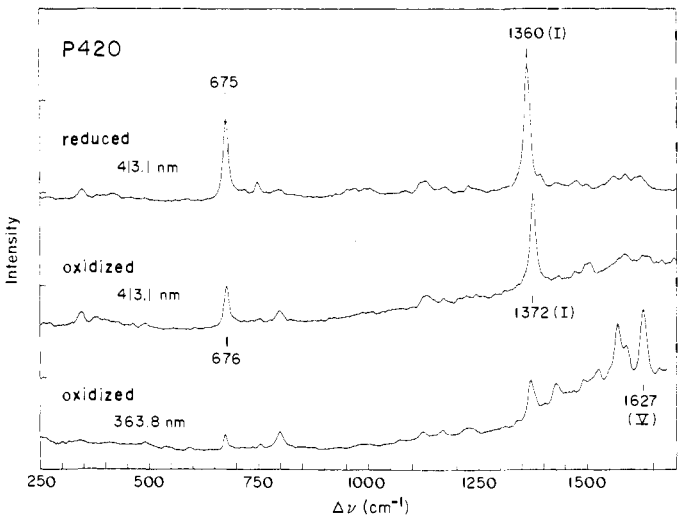

Figure 9. Resonance Raman spectra of the acetone inactivated P420 form of cytochrome *m*. Reduced P420, 413.1-nm excitation, 0-6K counts, parallel polarized scattering; oxidized P420, 413.1-nm excitation, 0-3.5K counts, parallel polarized scattering; oxidized P420, 363.8-nm excitation, 0-4.5K counts, unpolarized. The count ranges are equally extended and displaced as in Figure 3. The peak near 800 cm^{-1} is due to acetone.

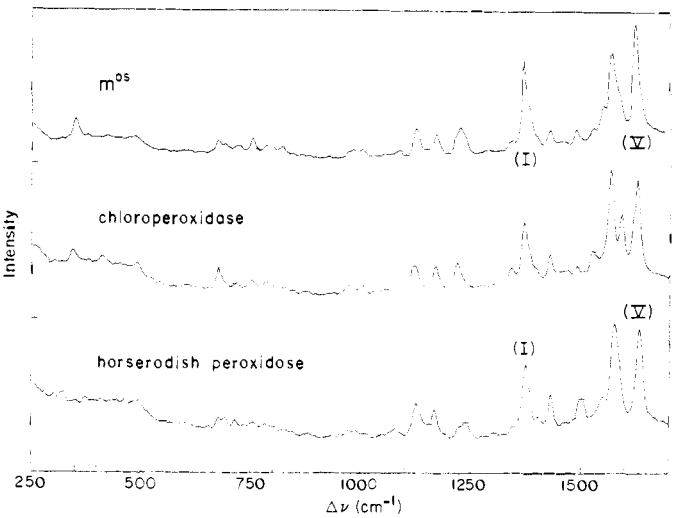

Figure 11. A comparative plot of the unpolarized resonance Raman spectra of m^{os}, native chloroperoxidase (ferric), and native horseradish peroxidase (ferric). All spectra are taken with 363.8-nm excitation and the experimental conditions are as in Figure 3. The count ranges are equally expanded and displaced: 0-5.5K counts for m^{os}; 0-5K counts for chloroperoxidase; 0-3K counts for horseradish peroxidase.

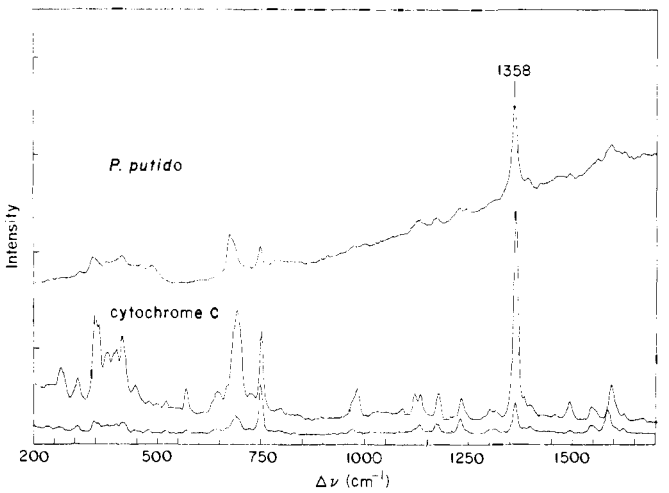

Figure 10. Resonance Raman spectrum of *Pseudomonas putida*, strain PpG 1, intact cells and, for comparison, ferrocytochrome *c* taken at 413.1 nm excitation. *P. putida* intact cells, 0-30K counts, unpolarized; ferrocytochrome *c*, 0-4.5K counts, parallel (upper) and perpendicular (lower) polarized scattering.

mentioned briefly as a candidate for an impurity species giving rise to the 1361-cm^{-1} peak in Figure 7. The enormous relative enhancements of the 675- and 1360-cm^{-1} modes of the ferrous sample with 413.1-nm excitation overpower all other modes in the spectrum. A similar dominance of bands at 676 and 1372 cm^{-1} is observed with 413.1-nm excitation of the oxidized state of P420. The positions of these strong, high-frequency bands at 1360 and 1372 cm^{-1} are typical for marker band I of ferrous and ferric hemeproteins.

Comparison of Raman spectra of the oxidized P420 species (Figure 9) to the m^{os} complex (Figure 3), when measured with 363.8-nm excitation, indicates the absence of 351- and 691-cm^{-1} modes in the P420 spectrum and small energy shifts of some high-frequency modes; the largest shift is observed for marker band V (dp), from 1623 cm^{-1} in m^{os} to 1627 cm^{-1} for P420. Table I contains a summary of the peak positions of oxidized P420. The absence of a 1627-cm^{-1} band in the 363.8-nm spectrum of m^{os} implies that there is very little, if any, P420 contamination of the m^{os} complex.

***Pseudomonas putida* Intact Cells.** The feasibility of observing resonance Raman spectra of the native camphor 5-monoxygenase system in vivo was explored by scattering off a dense paste of *Pseudomonas putida* cells positioned in a cooled container and sealed with a thin cover glass. Preliminary results are displayed in Figure 10. For comparative purposes a Raman spectrum of horse-heart ferrocytochrome *c*, measured with 413.1-nm laser excitation, is included in an attempt to indicate the contributions of other hemeproteins, including *c*-type cytochromes, functioning in electron transport and energy coupling pathways in *P. putida*. Differential excitation will be required to assign the spectral components of the individual hemeproteins in vivo. A systematic study has not been undertaken but the potential of the method is clear.

Other Hemeproteins. Figure 11 compares the resonance Raman spectra of m^{os}, chloroperoxidase, and horseradish peroxidase obtained with 363.8-nm laser excitation. All three hemeproteins contain iron in the high-spin ferric state thus allowing direct comparison of the spectra free from effects of valence and spin state. Some differences are apparent in the low-frequency modes below 500 cm^{-1}. The positions of the high-frequency marker bands, particularly bands I and V, are anomalously low in both m^{os} and chloroperoxidase when compared to the "normal" positions found in the spectrum of horseradish peroxidase. The spectra clearly contain detailed information about the active sites of these proteins that is of a more subtle nature than the valence and spin state of the central iron atom.

Discussion

One of the most significant results of this investigation is the observation of intense Raman modes in hemeproteins that are selectively enhanced by differential excitation within the Soret absorption band. The fluorescence background associated with visible excitation of cytochrome *m*, possibly due to impurities, is avoided and thus the resonance Raman modes in the various reaction states are revealed for the first time. Several earlier experiments have reported the use of laser lines close to Soret resonance but the dramatic enhancement of Raman intensities by excitation in *direct* resonance with the Soret peaks has not been previously exploited. A summary of the physical, chemical and biochemical information that can be drawn from these first

experiments follows: (1) A comparison of Raman spectral features of m^{os} and m^{rs} with other hemeproteins having the same valence and spin states indicates that the Raman marker bands can be quite sensitive to axial ligation. (2) The porphyrin π^* antibonding orbitals of m^{os} and m^{rs} contain an unusually large amount of electron density in the ground state due to increased π back-donation from the iron atom; this reflects the presence of a strong electron-donating axial ligand (such as mercaptide sulfur). (3) The Raman spectra of m^{os} and Pd$^o m^{os}$ provide an ambient temperature monitor of the heme iron spin-state equilibria in these complexes. (4) The excited state porphyrin macrocycle of m^o is expanded along normal coordinates corresponding to the 1372- and 676-cm^{-1} modes; the simultaneous enhancement of low-frequency Raman modes upon Soret excitation may reflect a change in iron-nitrogen equilibrium positions associated with the macrocycle expansion. (5) The observation of anomalous values of ρ_1 in the spectra of m^{rs} may indicate a lowered heme symmetry in this complex. (6) The low-frequency modes of m^o and m^{os} are selectively enhanced using excitation within the Soret absorption band; this fact along with experiments using ^{34}S-labeled cytochrome indicates that the 691-cm^{-1} mode of m^{os} is not due to the C–S stretching vibration of cysteine.

The following discussion is divided into four parts. The first section focuses on the high-frequency vibrations, 1300–1700 cm^{-1}, that have been assigned to porphyrin ring modes.[55] These frequencies have been found to depend in a characteristic way on the charge and spin state of the iron atom.[26] The second section discusses the low-frequency modes that are thought to involve the central iron atom and possibly the axial ligands; these modes have been less systematically studied and definitive assignments await comparison with isotopically modified samples. The third section discusses unusual features in the Raman spectra that are associated with the Soret resonance, while the final section correlates the Raman spectra with other physical probes and makes comparisons with other hemeproteins.

High-Frequency Marker Bands. The high-frequency porphyrin ring modes in cytochrome *m* differ considerably from the resonance Raman spectra of other hemeproteins.[36] The oxidation state marker band I (p), at 1368 cm^{-1} in m^{os} and 1344 cm^{-1} in m^{rs}, is shifted to lower frequency than found in most other high-spin ferric and ferrous heme complexes[36] (see Table III). The shift of band I in ferric m^{os} has been taken[32,35] to indicate a large (ground state) π^* population of the porphyrin ring due to the interaction of a strong electron-donating axial ligand, such as the mercaptide sulfur of cysteine. Similarly, the location of band I in the ferrous cytochrome provides the first evidence of mercaptide sulfur coordination to the heme in the m^{rs} complex.[40] Previous studies have supported mercaptide coordination in the m^{rs}_{CO},[18,41] m^{os},[19,20,42] and m^o [21,43] states.

The positions of the high-frequency marker bands II (p) and V (dp) are correlated to the spin state of the heme iron.[36] The shifts of band II, from 1502 to 1488 cm^{-1}, and of band V, from 1635 to 1623 cm^{-1}, are consistent with a transition from a low- to a high-spin ferric state on substrate association. A shoulder remaining at 1502 cm^{-1} in the m^{os} spectra indicates a residual low-spin species in the camphor bound complex. A mixture of high- and low-spin state species at 4 °C in the Raman spectra of m^{os} supports previous assignments of a temperature-dependent spin-state equilibrium in the substrate complex.[22,25,44] In addition the formation of a ternary complex (substrate, cytochrome and iron–sulfur effector protein) is accompanied by a decrease in intensity of the m^{os} band II at 1488 cm^{-1} (high-spin) relative to the 1502 cm^{-1} (low-spin) band, and thus reveals a high- → low-spin shift in the spin-state equilibrium. A decrease in the high-spin fraction of m^{os} on binding of the iron–sulfur protein, Pd^o, to form the Pd$^o m^{os}$ complex has previously been observed by optical,[45] electron spin resonance,[46] and Mössbauer[22] spectroscopies.

Table III. Marker Band Positions of Some Heme Proteins[a]

Hemeprotein	I (p)	II (p)	V (dp)
High-Spin Ferric			
Horseradish peroxidase	1375	1500	1630
Hemoglobin fluoride	1373	1482	1608
Cytochrome *c'*	1372	1500	1637
Chloroperoxidase	1369	1490	1627
Cytochrome m^{os}	1368	1488	1623
Low-Spin Ferric			
Horseradish peroxidase (CN^-)	1375	1497	1642
Hemoglobin cyanide (CN^-)	1374	1508	1642
Cytochrome *c* (Fe(III))	1374	1502	1636
Chloroperoxidase (CN^-)	1373	1503	1633
Cytochrome m^o	1372	1502	1635
High-Spin Ferrous			
Horseradish peroxidase (Fe(II))	1358	1472	1605
Deoxyhemoglobin	1358	1473	1607
Cytochrome *c'* (Fe(II))	1355	1475	1609
Chloroperoxidase (Fe(II))	1348	1470	1612
Cytochrome m^{rs}	1344	1466	1601 (?)[b]

[a] See ref 26, 35, 36, and 38. [b] See footnote 39.

Low-Frequency Modes. Laser excitation in resonance with the Soret band of cytochrome *m* resolves intense low-frequency vibrations. These vibrational modes are believed to be associated with the central iron atom.[28,47,48] The intensity enhancements of the low-energy modes in cytochrome *m* strongly depend on the position of the excitation wavelength within the Soret band of the several states. The strong 351-cm^{-1} mode of m^{os}, present with 363.8-nm excitation, disappears with 413.1-nm excitation and is replaced by at least four vibrations in the 300–450-cm^{-1} region. In the m^o spectra three low-energy modes are observed with excitation (413.1 nm) near the 417-nm Soret maximum while none are resolved with excitation at 363.8 nm. The differences in the low-frequency modes of the m^{os} and m^o states may reflect stereochemical or structural alterations at the heme active center associated with a change in spin state of the iron.[49,50]

The disappearance of the 351- and 691-cm^{-1} modes upon conversion of m^{os} to a P420 state has led to speculation that the 691-cm^{-1} band may arise from the 683-cm^{-1} C–S stretching vibration of cysteine.[32] This seems reasonable, particularly since axial ligand vibrations in heme model compounds have been recently reported[36] and out-of-plane *z*-polarized transitions have been identified at 323 and 567 nm in single crystal optical studies of m^{os}.[42] However, the anticipated frequency shift of the 691-cm^{-1} mode in ^{34}S-labeled m^{os} is not observed and assignment to a C–S stretching vibration cannot be made.[52] Selective enhancement of the low-frequency vibrations in the P420 state may account for the disappearance of these modes.

The low-frequency modes of the iron–sulfur protein, Pd^o, can be tentatively assigned by comparison with the resonance Raman studies of selenium-labeled adrenodoxin,[51] a $Fe_2S_2^*Cys_4$ protein with spectroscopic properties nearly indistinguishable from those of putidaredoxin. The strong vibrations at 287 and 394 cm^{-1} in Pd^o are assigned to vibrations associated with labile sulfur–iron modes and weaker vibrations centered around 340 cm^{-1} are consistent with cysteinyl sulfur–iron stretching modes.

Soret Band Resonance Enhancement. The relative intensities of the vibrational modes in m^{os} and m^o are strongly affected by the position of the laser excitation wavelength within the Soret band. The marker bands I, II, and V, the mode at ~675 cm^{-1}, and the modes below 500 cm^{-1} exhibit maximum in-

tensity enhancements at different excitation wavelengths. This selective enhancement of vibrations, using excitation within the Soret band, suggests that specific modes may derive their intensity from resonance with different electronic transitions. Potentially a great deal of information is contained in the Soret band excitation profile. The preliminary excitation profiles of the 676- and 1372-cm^{-1} (band I) modes of m^o provide the first quantitative evidence of resonance enhancement within the Soret transition.

The 676- and 1372-cm^{-1} modes of m^o are polarized ($\rho_l \simeq 1/8$ in D_{4h}) and presumably have A_{1g} symmetry. The symmetric A_{1g} vibrations are ineffective in vibronic mixing[53] and thus the two modes are consistent with resonance enhancement derived from an A-term contribution to the polarizability tensor.[31] Moreover, the analogous 1373-cm^{-1} mode of ferric hemoglobin fluoride has been shown to obey the A-term preresonance enhancement expected for a mode coupled to a single electronic transition.[54] The other A_{1g} modes in the m^o spectra are not so dramatically affected by resonance with the Soret transition. This enhancement pattern indicates that the excited electronic state associated with the Soret transition has an expanded porphyrin macrocycle stretched primarily along the normal coordinates corresponding to the 676- and 1372-cm^{-1} modes. The large vibrational overlap integrals (mixed Franck–Condon factors) necessary for strong A-term Raman scattering[31] appear for those modes with shifted excited state equilibrium positions and provide the selective A_{1g} enhancements. Normal mode calculations[55,56] have indicated that the 1372-cm^{-1} mode primarily involves breathing of the outer porphyrin ring. Assignment of the 676-cm^{-1} mode is not determined but may involve a symmetric in-plane bending vibration. Raman spectra of ^{15}N-enriched metallooctaethylporphyrins have indicated that the vibrational mode of the oxidation state marker (band I) includes appreciable contribution from the $C_\alpha N$ symmetric stretching vibration and is associated with ~0.01 Å in-phase displacement of the four pyrrole nitrogens toward the metal ion.[57] A change in the equilibrium position of the iron–nitrogen system, accompanying the porphyrin expansion in the excited state, may give rise to A-term enhancement of low-frequency iron–nitrogen vibrations. This could account for the relatively strong low-frequency bands in the m^o complex.

The spectra of the m^{rs} complex are also measured with excitation almost exactly in resonance with the Soret maximum. There is a substantial increase of $I_\perp$ for various modes that results in large values of ρ_l ($\rho_l \simeq 0.5$ for the 1344-cm^{-1} mode). The large ρ_l values may be due to dispersion effects. Dispersion in the depolarization ratio has been discussed for A_{2g} modes[58,59] and is predicted for B_{1g}, B_{2g}, and A_{1g} modes,[60] although the effect on the latter is expected to be quite small. Polarized spectra using nonresonant excitation of the m^{rs} complex are required to determine if dispersion accounts for the large values of ρ_l. Spectra measured with 488.0-nm excitation yield $\rho_l = 0.2$ for the 1344-cm^{-1} mode in m^{rs}.[40a] Large values of ρ_l could also be explained by lowering the D_{4h} symmetry assignment. A symmetry of D_{2h}, for example, will destroy the balance between x and y in the polarizability tensor and generate ρ_l values greater than 1/8 for A modes.[61] Very low symmetry at the iron atom has been detected in m^{rs} using Mössbauer techniques.[23]

Comparisons with Other Hemeproteins. It is useful to compare the Soret excited Raman spectra of cytochrome *m* with the spectra of other hemeproteins. For this purpose we list in Table III the positions of marker bands I, II, and V of a variety of hemeproteins. It is important to notice the similarities between the band positions of cytochrome *m* and chloroperoxidase in both the high-spin ferric and high-spin ferrous states. The marker band I in both of these proteins is found at an anomalously low position when compared to the other hemeproteins. This correlates well with data obtained from other physical probes[62,63] such as optical absorption, electron paramagnetic resonance, and Mössbauer spectroscopy which reveal similarities between the active sites of these two proteins that are not shared with other hemeproteins. In addition, Soret excited Raman spectra of m^{os} and native chloroperoxidase[35] indicate a low-spin minority species in both proteins and support previous observations[22,62] of temperature-dependent spin equilibria in these proteins. Some differences in the spectra of these two proteins do exist, particularly in the 1550–1600-cm^{-1} and the low-frequency regions, and indicate slight changes in the heme environment between oxidized (native) chloroperoxidase and m^{os}. However, positions of the main marker bands in both the oxidized and reduced high-spin species of each protein, along with other comparative physical–chemical data,[19,35,62,63] indicate that cytochrome *m* and chloroperoxidase have similar heme environments in these states and probably share the same axial ligand (the mercaptide sulfur of cysteine). These correlations in conjunction with Table III suggest that the anomalous position of band I may prove to be a useful diagnostic of cysteinyl axial ligand coordination in hemeproteins.

Acknowledgments. The authors are especially grateful to Professor Peter Debrunner for his critical reading of the manuscript and to Professor Aaron Lewis and Spectra Physics Inc. for their generous loan of equipment. We also wish to acknowledge the helpful advice of Professor A. C. Albrecht and Dr. L. Ziegler and the support of the Cornell Materials Science Center through NSF Grant DMR 76-01281. Additional support was provided in part by grants from the National Institutes of Health, AM00562 and AM20379, and the National Science Foundation, national needs postdoctoral fellowship (G.C.W.), SMI 77-12421.

References and Notes

(1) (a) Cornell University; (b) University of Illinois.
(2) D. Garfinkle, *Arch. Biochem. Biophys.*, 77, 493 (1958).
(3) M. Klingenberg, *Arch. Biochem. Biophys.*, **75**, 376 (1958).
(4) H. S. Schleyer, D. Cooper, S. Levin, and O. Rosenthal in "Biological Hydroxylation Mechanisms", G. Boyd and R. S. Smellie, Ed., Academic Press, New York, N.Y., 1972, p 187.
(5) A. Lu and M. J. Coon, *J. Biol. Chem.*, **243**, 1331 (1968).
(6) A. Lu, K. Junk and M. J. Coon, *J. Biol. Chem.*, **244**, 3714 (1969).
(7) A. H. Conney, *Pharmacol. Rev.*, **19**, 317 (1967).
(8) J. R. Gillette, *Adv. Pharmacol.*, **4**, 219 (1966).
(9) M. Katagiri, G. Ganguli, and I. C. Gunsalus, *J. Biol. Chem.*, **243**, 3543 (1968).
(10) I. C. Gunsalus, C. A. Tyson, R. Tsai, and J. Lipscomb in "Oxidases and Related Redox Systems", T. King, H. Mason, and M. Morrison, Ed., University Park Press, Baltimore, Md., 1973, p 583.
(11) I. C. Gunsalus and G. C. Wagner, *Methods Enzymol.*, in press.
(12) Abbreviations: *m*, cytochrome $P450_{CAM}$ monoxygenase; Pd, putidaredoxin; fp, putidaredoxin reductase. Oxidation and substrate association states indicated by superscripts, e.g., m^o, oxidized (ferric) cytochrome; m^r, reduced (ferrous) protein; and m^s, substrate bound camphor complex. Heme axial ligands at sixth coordination site indicated by subscripts, e.g., $m^{rs}_{O_2}$, ternary complex of dioxygen, substrate and reduced cytochrome *m*.
(13) I. C. Gunsalus and S. G. Sligar, *Adv. Enzymol.*, in press.
(14) I. C. Gunsalus, J. Meeks, J. Lipscomb, P. Debrunner, and E. Münck in "Molecular Mechanisms of Oxygen Activation", O. Hayaishi, Ed., Academic Press, New York, N.Y., 1974, p 559.
(15) D. Cooper, O. Rosenthal, R. Synder, and C. Witmer, Ed., *Adv. Exp. Med. Biol.*, **58** (1975).
(16) M. J. Coon, I. C. Gunsalus, and S. Maričić, Ed., *Croat. Chem. Acta*, **49**, No. 2 (1977).
(17) J. Stern and J. Peisach, *J. Biol. Chem.*, **249**, 7495 (1974).
(18) C. K. Chang and D. Dolphin, *J. Am. Chem. Soc.*, **98**, 1607 (1976).
(19) J. Dawson, R. Holm, J. Trudell, and S. C. Tang, *J. Am. Chem. Soc.*, **98**, 3707 (1976).
(20) S. C. Tang, S. Koch, G. Papaefthymiou, S. Foner, R. B. Frankel, J. A. Ibers, and R. H. Holm, *J. Am. Chem. Soc.*, **98**, 2414 (1976).
(21) M. Chevion, J. Peisach, and W. Blumberg, *J. Biol. Chem.*, **252**, 3637 (1977).
(22) M. Sharrock, P. G. Debrunner, C. Schulz, J. D. Lipscomb, V. Marshall, and I. C. Gunsalus, *Biochim. Biophys. Acta*, **420**, 8 (1976).
(23) P. M. Champion, J. Lipscomb, E. Münck, P. Debrunner, and I. C. Gunsalus, *Biochemistry*, **14**, 4151 (1975).
(24) P. M. Champion, E. Münck, P. Debrunner, T. Moss, J. Lipscomb, and I. C. Gunsalus, *Biochim. Biophys. Acta*, **376**, 579 (1975).
(25) R. Tsai, C. A. Yu, I. D. Gunsalus, J. Peisach, W. Blumberg, W. H. Orme-Johnson, and H. Beinert, *Proc. Natl. Acad. Sci. U.S.A.*, **66**, 1157 (1970).

(26) (a) T. Spiro, *Biochim. Biophys. Acta*, **416**, 169 (1975); (b) T. Yamamoto, G. Palmer, D. Gill, I. Salmeen, and L. Rimai, *J. Biol. Chem.*, **248**, 5211 (1973); (c) T. Kitagawa, Y. Kyogoku, T. Iizuka, and M. Saito, *J. Am. Chem. Soc.*, **98**, 5169 (1976).
(27) T. Spiro and T. Strekas, *Proc. Natl. Acad. Sci. U.S.A.*, **69**, 2622 (1972).
(28) S. Asher and K. Sauer, *J. Chem. Phys.*, **64**, 4115 (1976).
(29) M. Gouterman, *J. Mol. Spectrosc.*, **6**, 138 (1961).
(30) G. C. Wagner and R. J. Kassner, *Biochem. Biophys. Res. Commun.*, **63**, 385 (1975).
(31) J. Tang and A. C. Albrecht in Raman Spectroscopy", Vol. 2, H. Szymanski, Ed., Plenum Press, New York, N.Y., 1970, p 33.
(32) P. M. Champion and I. C. Gunsalus, *J. Am. Chem. Soc.*, **99**, 2000 (1977).
(33) G. K. Garg, I. C. Gunsalus, W. Toscano, and G. C. Wagner, *J. Biol. Chem.*, in press.
(34) C-A. Yu and I. C. Gunsalus, *J. Biol. Chem.*, **249**, 102 (1974).
(35) (a) R. Remba, P. M. Champion, R. Chiang, D. Fitchen, and L. P. Hager, *Biochem. Biophys. Acta*, in press; (b) P. M. Champion, R. Remba, R. Chiang, D. B. Fitchen, and L. P. Hager, *ibid.*, **446**, 486 (1976).
(36) T. Spiro and J. Burke, *J. Am. Chem. Soc.*, **98**, 5482 (1976).
(37) $I_\parallel$ and $I_\perp$, scattered Raman intensity polarized parallel and perpendicular, respectively, to the incident radiation; $\rho_l = I_\parallel/I_\perp$, depolarization ratio; p, polarized; dp, depolarized; ap, anomalously polarized.
(38) (a) T. Spiro and T. Strekas, *J. Am. Chem. Soc.*, **96**, 338 (1974); (b) L. Rimai, I. Salmeen, and D. Petering, *Biochemistry*, **14**, 378 (1975).
(39) Assignment of the 1601-cm^{-1} mode to band V is still open to question because spectra with visible excitation have not been obtained.
(40) (a) Y. Ozaki, T. Kitagawa, Y. Kyogoku, H. Shimada. T. Iizuka, and Y. Ishimura, *J. Biochem.* (*Tokyo*), **80**, 1447 (1976). (b) A similar conclusion about the axial coordination in the m^s state was reached independently by these authors, whose work was brought to our attention during preparation of this manuscript.
(41) L. K. Hanson, W. Eaton, S. Sligar, I. C. Gunsalus, M. Gouterman, and C. R. Connell, *J. Am. Chem. Soc.*, **98**, 2672 (1976).
(42) L. Hanson, S. Sligar, and I. C. Gunsalus, *Croat. Chim. Acta*, **49**, 237 (1977).
(43) W. E. Blumberg and J. Peisach in "Structure and Function of Macromolecules and Membranes", Vol. 2, B. Chance, Ed., Academic Press, New York, N.Y., 1971, p 215.
(44) S. G. Sligar, *Biochemistry*, **15**, 5399 (1976).
(45) S. G. Sligar, Ph.D. Thesis, University of Illinois, 1975.
(46) J. Lipscomb, Ph.D. Thesis, University of Illinois, 1974.
(47) H. Ogoshi, Y. Saito, and K. Nakamoto, *J. Chem. Phys.*, **57**, 4194 (1972).
(48) H. Brunner and H. Sussner, *Biochim. Biophys. Acta*, **310**, 20 (1973).
(49) M. F. Perutz, *Nature* (*London*), **228**, 726 (1970).
(50) J. L. Hoard, *Science*, **174**, 1295 (1971).
(51) S. Tang, T. Spiro, K. Mukai, and T. Kimura, *Biochem. Biophys. Res. Commun.*, **53**, 869 (1973).
(52) One ambiguity remains unexplained. The first Raman spectrum measured of the ^{34}S-labeled m^{os} complex displayed two well-resolved peaks at 675 and 687 cm^{-1}. This result was never reproduced in the many spectra that followed and must be considered invalid. Additional measurements of crystallized ^{34}S m^{os} samples are planned to obtain higher quality spectra, but observation of a shift in the 691-cm^{-1} mode appears unlikely.
(53) M. Perrin, M. Gouterman, and C. Perrin, *J. Chem. Phys.*, **50**, 4137 (1969).
(54) T. Strekas, A. Packer, and T. Spiro, *J. Raman Spectrosc.*, **1**, 197 (1973).
(55) P. Stein, J. Burke, and T. Spiro, *J. Am. Chem. Soc.*, **97**, 2304 (1975).
(56) S. Sunder and H. Bernstein, *J. Raman Spectrosc.*, **5**, 35 (1976).
(57) T. Kitagawa, M. Abe, Y. Kyogoku, H. Ogoshi, H. Sugimoto, and Z. Yoshida, *Chem. Phys. Lett.*, **48**, 55 (1977).
(58) D. W. Collins, D. B. Fitchen, and A. Lewis, *J. Chem. Phys.*, **59**, 5714 (1973).
(59) D. W. Collins, P. M. Champion, and D. B. Fitchen, *Chem. Phys. Lett.*, **40**, 416 (1976).
(60) D. W. Collins, private communication.
(61) W. M. McClain, *J. Chem. Phys.*, **55**, 2789 (1971).
(62) P. M. Champion, E. Münck, P. G. Debrunner, P. Hollenberg, and L. P. Hager, *Biochemistry*, **12**, 426 (1973).
(63) P. M. Champion, R. Chiang, E. Münck, P. Debrunner, and L. P. Hager, *Biochemistry*, **14**, 4159 (1975).

Microwave, Infrared, and Raman Spectra, Conformation, Dipole Moment, and Vibrational Assignment of Ethyldifluoroborane

J. D. Odom,* Y. S. Li, E. J. Stampf, and J. R. Durig*

Contribution from the Department of Chemistry, University of South Carolina, Columbia, South Carolina 29208. *Received November 28, 1977*

Abstract: The microwave spectra of $CH_3CH_2{}^{10}BF_2$ and $CH_3CH_2{}^{11}BF_2$ have been recorded from 26.0 to 40.0 GHz. A-type transitions were observed and R-branch assignments have been made for the ground vibrational state for both ^{10}B and ^{11}B and four excited states of the $^{11}BF_2$ torsion. B-Type transitions were also assigned for the ground and first excited state of the $^{11}BF_2$ torsion. From the small value of $I_a + I_b - I_c = 6.318$ amu Å^2, it is concluded that the major conformation of ethyldifluoroborane has all heavy atoms coplanar and that this quantity arises mainly from the four out-of-plane hydrogens of the ethyl moiety. The total dipole moment was determined to be 1.69 ± 0.02 D, with components $\mu_a = 1.15 \pm 0.02$ D and $\mu_b = 0.75 \pm 0.02$ D. The infrared (20-3500 cm^{-1}) and Raman spectra (0-3500 cm^{-1}) have been recorded for both the gas and solid. Additionally, the Raman spectrum of the liquid was recorded and qualitative depolarization values obtained. The BF_2 internal torsional mode was observed at 44 cm^{-1} in the infrared spectrum of the gas and a twofold periodic barrier of 1.17 kcal/mol was calculated. These data are consistent with the relative intensity measurements in the microwave spectrum. The structural results are compared with previous ab initio calculations for ethylborane in which the most stable conformation is a staggered structure. The barrier to internal rotation of the BF_2 moiety is also compared to that of the isoelectronic molecule nitroethane which exhibits free rotation of the nitro group. The B-C bond distance of 1.572 Å appears reasonable relative to the values reported for this distance in other organoboranes.

Introduction

In general there has been very little structural information reported for organoboron compounds, particularly gas-phase determinations.[1] Recently we have initiated a program to investigate the spectra and structure of organoboranes.[2-8] A structural study of the vinyldifluoroborane molecule[3,8] included the microwave spectra of 15 isotopic species as well as the complete assignment of the infrared and Raman spectra. The molecule was planar and had a twofold barrier to internal rotation of 4.17 kcal/mol. As a continuation of these studies, we have investigated the infrared, Raman, and microwave spectra of ethyldifluoroborane, $C_2H_5BF_2$.

Dill et al.[9] recently reported a theoretical study of the energies and conformations of a series of XCH_2Y molecules which included ethylborane, $CH_3CH_2BH_2$. Ab initio molecular orbital theory predicts[9] the conformation of this hypothetical molecule to have the BH_2 group staggered with respect to the methyl moiety (i.e., the methyl group bisects the HBH angle) with a B-C rotational barrier of 0.2 kcal/mol. We felt that a determination of the conformation and barrier to in-

0002-7863/78/1500-3751$01.00/0